Latin American Journal of Solids and Structures
www.lajss.org

Numerical study of the influence of the specimen geometry on split Hopkinson bar tensile test results

Abstract

Finite element simulations of high strain rate tensile experiments on sheet materials using different specimen geometries are presented. The simulations complement an experimental study, using a split Hopkinson tensile bar set-up, coupled with a full-field deformation measurement device. The simulations give detailed information on the stress state. Due to the small size of the specimens and the way they are connected to the test device, non-axial stresses develop during loading. These stress components are commonly neglected, but, as will be shown, have a distinct influence on the specimen behaviour and the stress-strain curve extracted from the experiment. The validity of the basic assumptions of Hopkinson experiments is investigated: the uniaxiality of the stress state, the homogeneity of the strain and the negligibleness of the deformation of the transition zones. The influence of deviations from these assumptions on the material behaviour extracted from a Hopkinson experiment is discussed.

Keywords

Hopkinson, specimen geometry, deformation, stress-strain curve, high strain rate testing, numerical simulation, steel sheet

Patricia Verleysen*, Verhegghe Benedict, Tom Verstraete and Degrieck Joris

Department of Materials Science and Engineering, Ghent University, Faculty of engineering, Sint-Pietersnieuwstraat 41, Belgium, 9000 Gent, tel. 32-9-264.34.35, fax. 32-9-264.35.87

Received 29 Jun 2009;
In revised form 5 Aug 2009

* Author email: Patricia.Verleysen@UGent.be

1 INTRODUCTION

The use of split Hopkinson bar set-ups to study the impact-dynamic mechanical properties of materials has increased considerably in recent years [5]. Although split Hopkinson bar facilities exist for high strain rate bending, shearing and torsion, the technique is most often used for tensile and compression testing. For compression tests cylindrical specimen are subjected to the high strain rate loading. For split Hopkinson tensile bar (SHTB) experiments dogbone-shaped specimens, consisting of a central zone with a constant cross-section and two transition zones in which the cross-section gradually increases, are used. In literature widely divergent dimensions for the length and width of the central zone, and the specific shape and dimensions of the transition zones can be found.

It is generally assumed that a Hopkinson experiment yields the material behaviour. However, the experimental study presented in [4] clearly demonstrates that the geometry has a

non-negligible influence on the stress-strain curves extracted from the experiments. The classical measurement and processing technique is based on assumptions related to the specimen deformation: 1) the transition zones do not contribute to the total specimen deformation, all deformation is concentrated in the central zone, and 2) stresses and strains are homogeneous in the central zone. For the material considered in [4] it is proved that these assumptions are not only far from being fulfilled, but give in addition rise to erroneous deformation values.

High-quality experiments are fundamental for material research. However, experimental studies have some inherent shortcomings which often impede an in-depth understanding of the observed phenomena. The experimentally established material behaviour is the result of a complex interaction of numerous parameters. To estimate the influence of each single parameter an elaborate series of experiments is required. Additional difficulties will arise because some tendencies are masked by unavoidable scatter on the experimental results and/or measurement inaccuracies, and the limited possibilities of the measurement techniques currently available. These shortcomings can be overcome by numerical simulations. Indeed, by means of simulations, the influence of the material behaviour and of parameters related to the experimental setup, such as the specimen geometry, the bar-specimen connection and the Hopkinson bars (diameter and material), on the stress-strain distribution in the specimen can be isolated and thoroughly studied without having to go through a series of time-consuming experiments.

In this paper results are presented of finite element simulations of SHTB experiments on a steel sheet. The emphasis is laid on the influence of the geometry on the specimen behaviour during an experiment. Seven dogbone-shaped geometries are considered. The considered steel specimen has mechanical properties corresponding with a TRansformation Induced Plasticity (TRIP) steel. Second order geometrical influences resulting from the strain rate and adiabatic specimen heating are neglected.

As will be shown, as a result of the connection of the specimen with the bars and the bone-shaped geometry of the specimen, non-axial stresses develop during loading. These non-axial stress components have a non-negligible influence on the specimen behaviour and thus the stress-strain curve extracted from the experiment; the onset of yielding, the stress corresponding to a certain level of deformation, the homogeneity of the stress and deformation are all affected by the specimen geometry.

The authors should emphasize the fact that the deviations between the material behaviour and extracted behaviour established in this contribution are not due to erroneous and/or inaccurate signal processing. Indeed, only the influence of the specimen geometry on the stress-strain curve extracted from the experiments is discussed; errors induced by the shifting of the waves towards the specimen interfaces (wrong time, neglecting Pochhammer-Cree oscillation [3]) are excluded.

2 SPLIT HOPKINSON TENSILE BAR EXPERIMENT

2.1 Assumptions

During a SHTB experiment a material sample is fixed between two Hopkinson bars: an input bar and an output bar. The specimen is subjected to a high strain rate tensile load through the interaction of a tensile wave, generated at the free end of the input bar, with the specimen. The incident wave is partly reflected and partly transmitted by the specimen. The strain histories ϵi(t), ϵr(t) and ϵt(t) corresponding to respectively the incident, reflected and transmitted wave are measured at well chosen points on the Hopkinson bars. After shifting the waves towards the specimen/bar interfaces, the stress, the strain and the strain rate in the specimen can be calculated using the following expressions [1]:

$$\begin{aligned} \sigma(t) &= \frac{A_b E_b}{A_s}\varepsilon_t(t) \\ \varepsilon(t) &= \frac{U_{ob} - U_{ib}}{L_s} = -\frac{2C_b}{L_s}\int_0^t \varepsilon_r(\tau)d\tau \\ \dot{\varepsilon}(t) &= \frac{V_{ob} - V_{ib}}{L_s} = -\frac{2C_b}{L_s}\varepsilon_r(t) \end{aligned} \tag{1}$$

with E_b the modulus of elasticity of the Hopkinson bars, A_s and A_b the cross section area of the specimen and of the Hopkinson bars respectively, C_b the velocity of propagation of longitudinal waves in the Hopkinson bars and L_s the gage length of the specimen. U_{ib} and U_{ob} are the displacements of the interface between the specimen and, respectively, the input bar and the output bar; V_{ib} and V_{ob} are the corresponding velocities.

Equations (1) are based on the assumption that in the specimen a quasi-static equilibrium is established. Inertial forces acting on the specimen are omitted; the tensile forces at the interfaces of the specimen with the input bar and output bar, and consequently in each transverse section of the specimen, are equal. In the zone of the specimen where a constant cross-section exists stresses, as well as strains and strain rates, are considered to be homogeneous. Moreover, stresses are assumed to be uniaxial in this zone. Finally, the deformation of the transition zones, where the section of the specimen is changing, is neglected.

2.2 Specimen geometry

A schematic representation of the specimen geometry is given in Fig. 1. It consists of a central zone with a constant width and a certain length, and, on both ends of the central zone, transition zones where the width gradually increases following a circular curve. The zones of the specimen shaded in Fig. 1 are needed to glue the specimen in slits at the ends of the Hopkinson bars.

As discussed in [4], the dimensions of the reference geometry are established based on geometries described in literature: the length of the central zone is 5 mm, the width of this zone is 4 mm, and the radius of the transition zones is 2 mm. Starting from that reference geometry, six additional geometries are determined by varying the radius of the transition

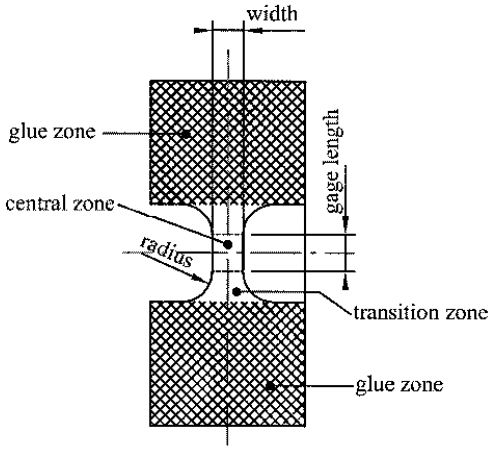


Figure 1 Schematic representation of the specimen geometry.

zones, the length and the width of the central zones. Each time only one parameter is changed while the other two remain constant (see table 1). Accordingly, the influence of the radius of the transition zones (geometry 3 and 4), the length (geometry 5 and 6) and the width of the cross-section (geometry 2 and 7) can be studied.

Table 1 Dimensions of the geometries considered in this study. Geometry 1 is the reference geometry; dimensions deviating from the reference geometry are in bold.

Geometry	Length (mm)	Width (mm)	Length/Width	Radius
1	5	4	1.25	2
2	5	**6**	**0.83**	2
3	5	4	1.25	**1**
4	5	4	1.25	**4**
5	**10**	4	**2.5**	2
6	**3.33**	4	**0.83**	2
7	5	**2**	**2.5**	2

3 FINITE ELEMENT MODEL

The numerical simulations were performed using the finite element program ABAQUS (from ABAQUS, Inc.). The finite element model was created with ABAQUS/CAE. Since we wanted to study the precise dynamical phenomena in the specimen, we used the ABAQUS/Explicit code for the calculations.

To correctly take into account inertia and wave propagation phenomena, the interaction of a real wave with the specimen is modelled. The model comprises the test specimen and parts of both Hopkinson bars long enough to have no interference of reflected stress waves with the

specimen during the time period of interest. Bars of 2 m length were sufficient. Because of the symmetry only one quarter of the cross-section was modelled, and symmetry conditions imposed.

The different specimen geometries (see section 2) and the Hopkinson bars were created as separate parts in Abaqus/CAE, and subsequently assembled. A test specimen was connected to the Hopkinson bars by a tied interface on the side surfaces only. The butt of the specimen was not tied to the Hopkinson bar, as it is unlikely that the glue can transmit the high stresses that would result. Loading on the model is applied as a stress wave on the end of the input Hopkinson bar. The stress wave used was derived from strain gauge readings on the input bar of the incident wave during a real test. For the specimens a classical metal, elasto-plasticity model with isotropic hardening was used. Tabulated data were entered, corresponding to the stress-strain relationship in Fig. 2, which was established during a static tensile experiment on an Al-TRIP steel [2].

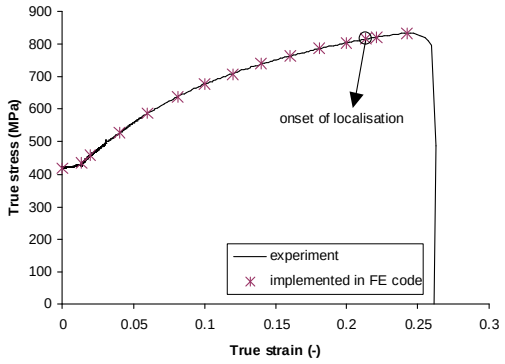


Figure 2 Experimentally established stress-strain curve of an Al-TRIP steel implemented in the finite element program.

A finite element mesh was generated with 4 elements through the (half) thickness of the specimen, see Fig. 3. The mesh is finer in the smaller section of the specimen, where elements are approximately cubes. The Hopkinson bars were meshed quite coarser, since they are not of interest for our study and only serve to transmit the loading on the specimen. The element type used is C3D8R, an eight node linear brick type element using reduced integration with hourglass control. This is the obvious choice for modelling 3D solids under highly dynamic conditions. The element mesh for the specimen in the figure comprises 14060 nodes and 10528 elements. Each of the Hopkinson bars accounted for approximately 34005 nodes and 25957 elements. Total runtime including data check and full analysis was about 6 hours.

4 RESULTS

In this section the development of stresses and strains in the Hopkinson specimens during loading is briefly discussed with emphasis on those issues important for the material behaviour extracted from a Hopkinson experiment (see section 5).

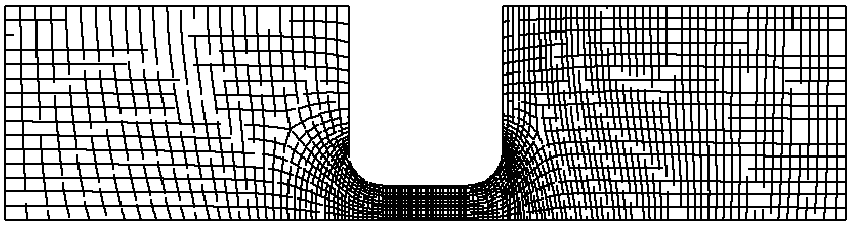


Figure 3 Finite element model of the specimen.

Phase of elastic deformation

From the onset of loading, stresses and strains in the specimen are reversible until at a certain moment plastic deformation starts. For all geometries, the elastic limit is initially exceeded at the outside borders of the transition zones, close to the central zone. During elastic deformation, the highest value of the axial stress is reached at the outside border near the transition between the central zone and the curved section. Non-axial stresses are caused by 1) the bending of the forcelines due to the changing cross-section of the specimen in the transition zones and by 2) the limitation of the Poisson deformation perpendicular to the loading direction by surrounding material and Hopkinson bars. The first cause is dominant; the highest non-axial stresses are reached at the shoulders of the specimen. At the moment that plastic deformation starts at the shoulders, a drop in non-axial stress can be noticed around the centre of the specimen.

Phase of early plastic deformation

Very soon after the onset of plastic deformation at the border of the transition zones, yielding also starts in the centre of the specimen. Geometry 5 is an exception: here yielding in the central zone starts in two points at a certain distance from (but symmetrical around) the centre of the specimen. Very soon afterwards, the zones join to constitute one zone around the centre of the specimen. For all geometries, the large differences in deformation magnitudes between the elastically and plastically deforming material give rise to additional stresses near the borders of the plastically deformed regions. Since several plastically deformed zones exist, during this phase complex stress and strain states are obtained. Both the plastically deformed zones in the transition zones and the one in the central zone propagate and finally merge to constitute single zone of plastic deformation.

Phase of stable plastic deformation

During stable yielding the plastic deformation spreads in the transition zones towards the specimen/bar interfaces. During this phase a more conventional stress and strain distribution is obtained in the specimen. In a zone around the middle of the specimen fairly homogeneous axial stresses and strains exist. For most geometries, non-negligible non-axial stresses exist in the specimen, even in the central zone. The non-axial stresses in the centre of the specimen are mainly determined by the length to width ratio: the smaller this ratio, the higher the non-axial stresses. In second order also the radius of the transition zones intervenes: if geometry 1, 3

and 4 are compared, it is clear that the higher the radius, the smaller the non-axial stresses. Non-axial stresses increase from the centre towards the transition zones. The more to the end of the central zone, the more the influence of the radius and the width of the specimen as such becomes clear.

Phase of strain localisation

In this final stage deformation will localise in a zone around the middle of the specimen. Since, softening of the material is not included in the material model implemented in the FE-code, only the start of this final stage is correctly predicted by the simulations.

During all phases, considerable non-axial tensile stresses exist in the transition zones. These stresses reduce the axial deformation of the transitions zones and consequently have a favourable effect on the deformation extracted from a Hopkinson experiment. The presence and evolution of non-axial stresses in the central zone on the contrary has an adverse influence on the homogeneity of the axial stress and strain in the central zone.

5 ANALYSIS

5.1 Stress history in the specimen

The stress-strain curve calculated from the signals recorded during a Hopkinson experiment is assumed to represent the uniaxial material behaviour. However, two fundamental objections raise from the discussion in section 4:

- non-axial stresses exist in the specimen, even in central zone; the specimen behaviour will consequently deviate from the uniaxial behaviour,
- stresses and strains in the central zone are influenced by the transition zones and even by the material and diameter of the Hopkinson bars; a structural response and not a material response is thus obtained.

To estimate the influence of these objections on the stress-strain relation extracted from a Hopkinson experiment, the material law implemented in the FE-code, which represents the uniaxial material behaviour, is compared with the actual axial stress-strain relation established in the centre of the specimen in Fig. 4. Clear deviations between the material law and the curves for the different geometries are obvious during all phases of the deformation.

It is interesting to note that the slope of the stress-strain curve in the centre during elastic deformation varies from 206.9GPa for geometry 5 to 211.0GPa for geometry 2, while the implemented modulus of elasticity is 208GPa. Due to the (small) non-axial compressive stresses in geometry 5, the material apparently behaves less stiff than materials where non-axial tensile stresses exist.

Another interesting observation is that the slope of the stress-strain curve in Fig. 4 decreases before the actual onset of yielding in the centre. Indeed, as mentioned in section 4, at the moment that yielding starts at the transition zones a drop in the non-axial stress in the centre

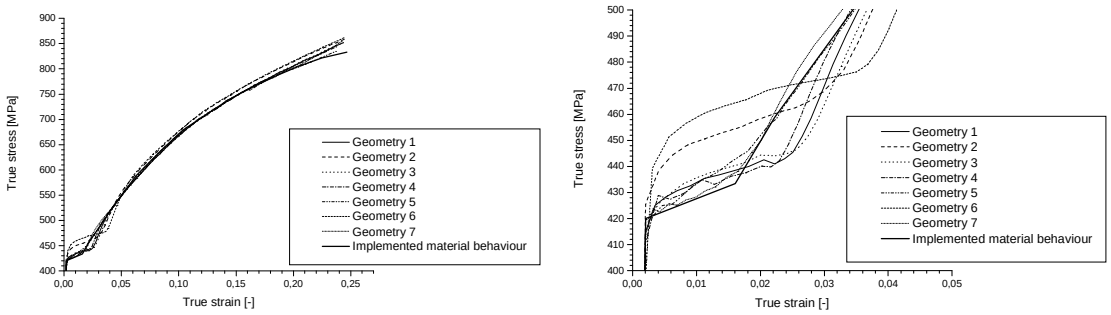


Figure 4 (a) Stress-strain curve in the centre of the specimen for the seven geometries, and the material law used for the simulations. (b) Detail of the stress-strain curve in the centre of the specimen.

occurs, and as a result the slope of the stress-strain curve decreases. When the stress-strain curve of geometry 2 is observed in Fig. 4b, a first change in slope can be observed at a stress level of 425MPa, however actual yielding in the centre only starts at a stress level of 439MPa. Consequently, the decrease in the slope of the stress strain curve does not necessarily indicate the onset of yielding, and can consequently not be used for that purpose.

After the onset of yielding, a plateau appears in the implemented stress-strain curve: an increase of the stress from 420 to 433.4MPa gives rise to a strain increase of more than 1.4%. During the early stage of yielding the simulated stress-strain curves also exhibit a part with lower slope (Fig. 4b), however, it is clear that the corresponding stress levels and deformations are strongly geometry dependent:

- For all geometries higher plateau stress values are reached, in geometry 6 for example, the first plastic strain appears at an axial stress of 440MPa; this is, compared with the value of the material law (420MPa), an overestimation of 4.8%. The value of the non-axial stress at the end of the elastic deformation accounts for the deviation: the higher the non-axial stress, the higher the initial yield stress.

- The deformation corresponding with the end of the plateau also varies. The largest value is again found for geometry 6, followed by geometry 2. The difference between the geometries are due to the structural behaviour of the specimens: the growth of the plastically deformed zone gives rise to a geometry dependent decrease in non-axial stress level, through which the deformation in the centre increases without significant increase of the axial stress level.

Since axial deformations are limited by non-axial tensile stresses, and facilitated by compressive stresses, during stable yielding non-axial stresses are again decisive. Compared to the other geometries, the axial deformation of geometries 1, 3 and 4 grows faster during the beginning of stable yielding when non-axial stresses are negative. However, soon after the non-axial stresses become positive, the stress at a certain strain level exceeds the implemented stress.

Geometries where considerable non-axial tensile stresses exist, such as geometry 2 and 6, intersect and exceed the implemented stress-strain curve soon after the onset of stable yielding. Since high non-axial tensile stresses develop in all geometries around strain localisation, all curves, except 5, end above the implemented material behaviour. In order of increasing tensile stress the geometries can be ordered as follows: geometry 5, geometry 7, geometry 4, close to geometry 1, close to 3 and finally geometry 2 and then geometry 6.

5.2 Homogeneity of stress and strain

Generally, it is assumed that in the central zone of the specimen homogeneous stresses and strains are obtained. However, from the simulations it is clear that both the axial stress and the axial strain are far from constant. The stress homogeneity is less critical than the strain homogeneity. The degree of non-homogeneity can be due to:

1. the fact that no state of quasi-static equilibrium is established in the specimen. Indeed, after the incident wave reaches the specimen, quasi-static equilibrium is reached after a certain time, related to the time needed for a wave to travel back and forth in the specimen, and thus to the wave propagation velocity in the specimen and the length of the specimen,

2. the existence and distribution of non-homogeneous non-axial stresses in the central zone of the specimen.

For the geometries and material considered here, the first effect is negligible. To quantify the homogeneity along the length of the specimen, the notion 90%-zone is introduced; it gives the length of the zone along the axis of the specimen where the strain is higher than 90% of the strain in the centre of the specimen. In Fig. 5 the evolutions of the 90%-zones as a function of the axial strain in the centre of the specimen are given for the seven geometries. As could be expected, the highest values of the 90%-zone are reached during elastic deformation. At the onset of plastic deformation in the centre of the specimen a sharp fall can be noticed. When the plastic deformation spreads, the 90%-zone rises again; a maximum is reached at the moment that the plastic deformation spreading from the middle of the specimen meets the plastic zones around the shoulders of the specimen. During the stage of stable plastic deformation, the 90%-zone gradually decreases. The oscillations that can be observed in the curve of geometry 5 are due to plastic waves travelling back and forth in the specimen.

When the values of the 90%-zones of geometries 1, 2, 3, 4 and 7 are compared, it is clear that, although their gage lengths are equal, more or less considerable differences exist between their 90%-zones. Equally, differences between the 90%-zones of geometries 1, 5 and 6 do not exactly correspond to the differences between their respective gage lengths. The value and distribution of the non-axial stresses in the central zone of the specimen account for the inferior correspondence between the gage length and the 90%-zone. Indeed, non-axial stresses have an adverse effect on the strain homogeneity. Since the specimen's length to width ratio mainly determines the non-axial stresses in the central zone, this ratio is also crucial for the

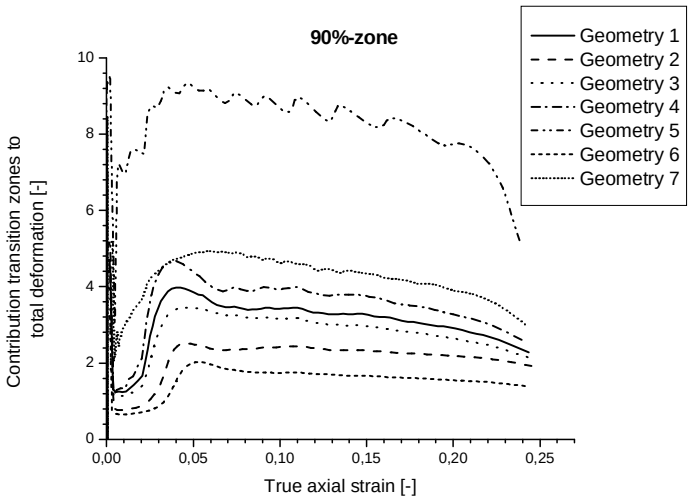


Figure 5 90%-zone as a function of the strain in the centre of the specimen for all geometries

homogeneity. At 10% axial strain in the centre of the specimen, the high length to width ratio geometries 5 and 7 have a 90%-zone equal to 86.8 and 92.5% of their respective gage lengths. Whereas for the medium length to width ratio geometries these percentages vary from 63.2 for geometry 3 over 68.4 for geometry 1 to 78.7 for geometry 4, thus indicating that the sharper the transition zones, the lower the 90%-curve. For the low length to width geometries 2 and 6 the 90%-zones are merely 48.2% and 52.2% of the gage length respectively. During plastic deformation of the specimen, the 90%-zone of geometry 6 varies from 2.02 to less than 1.4mm at strain localisation. The highest stresses and strains are confined to a small region across the centre of the specimen.

5.3 Classical strain calculation

The strain obtained by equation (1), referred to as *classical* strain, is assumed to represent the mean strain in the central zone of the specimen. In this section the ability of the classical strain to yield information on the actual deformation behaviour of the specimen will be discussed. Since it is the explicit intention to study the influence of the specimen geometry on the accuracy of the strain measurement, all factors that can induce non-geometry related errors are excluded. To avoid influences of erroneous and/or inaccurate signal processing such as incorrect time shifting of the waves or the neglect of Pochhammer-Cree oscillations in the shifting process, the classical strain is calculated by dividing the relative displacement of the bar/specimen interfaces by the length of the central zone and is thus in agreement with the first part of equation (1) for the strain. Important to note is that in this section engineering values are used, because it enables a more straightforward comparison between the classical (engineering) and simulated strains.

As discussed in section 5.2, the strain at a certain moment in the central zone is not constant, consequently the strain in the central zone does not exist. However, in a limited zone around

the centre of the specimen, more or less homogeneous stress and strain fields are established. In this zone the uniaxial, homogeneous stress state aimed at in a SHTB experiment is the most closely approximated; plastic deformation, strain localisation and final fracture will here occur. Both the extent of this zone and the degree of stress uniaxiality are strongly geometry dependent.

The stress, strain and strain rate arising in this zone provide information on the material behaviour of the specimen and are therefore of major importance. Consequently, the values of the stress and strain in or around the centre of the specimen are paramount over the mean stress and strain in the central zone. Accordingly, in this section the correspondence of the classical strain with the strain in the centre of the specimen, more than the correspondence with the mean strain in the central zone is used as criterion to assess the value and accuracy of the classical strain measurement.

By using equation (1) to calculate the classical strain, the assumed negligible deformation of the transition zones is added to the deformation of the central zone. From the experiments [4] as well as from the simulations, it is clear that, unlike what is commonly assumed, the deformation of the transition zones accounts for an important part of the total deformation. In Fig. 6 the relative contribution of the transition zones to the total deformation is represented for all geometries. The highest values are reached during elastic deformation. In descending order the geometries can be ordered as follows: geometry 4, 6, 2, 1, 7, 3 and finally 5. Values ranging from 55.3% for geometry 4 to 23.9% for geometry 5 are reached.

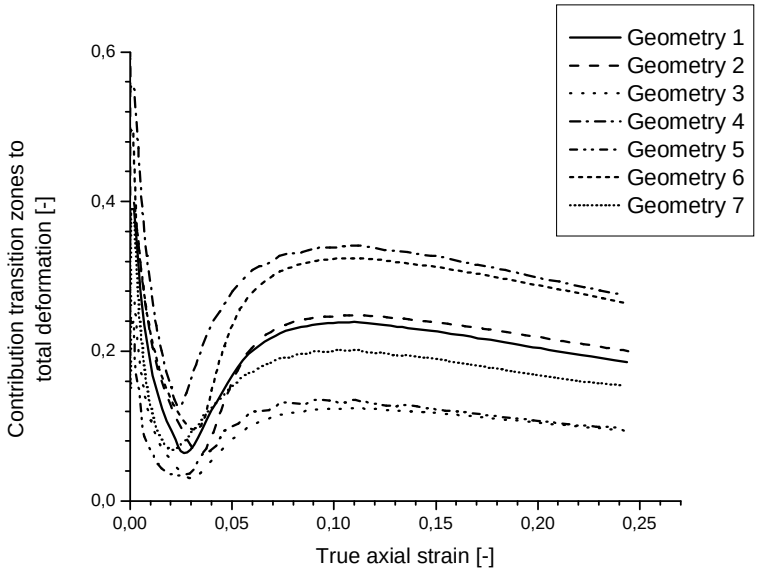


Figure 6 Relative contribution of the deformation of the transition zones to the total specimen deformation as a function of the strain in the centre of the specimen for all geometries

As soon as plastic deformation starts in the centre of the specimen, the relative contribution of the transition zones drops. When also the transition zones plastically deform, the relative contribution again increases to reach a maximum, approximately, and geometry dependent, at

a strain level of 10% in the centre of the specimen. Then, until rupture of the specimen, the relative importance of the deformation of the transformation zones steadily decreases. Ordered according to the contribution of the transition zones, during plastic deformation only geometry 3 and 5 switch places compared to the elastic phase. The transition zones of geometry 4 take up to 34.1% of the total deformation, only up to 12.4% for geometry 3.

In Figs. 7a and 7b the evolution of the strain along the axis of respectively geometry 3 and 6 are represented at the moment that approximately 10% strain is reached in the centre. In these figures the classically assumed strain evolution, zero in the transition zones and constant in the central zone, is also given. By neglecting the deformation of the transition zones, the classical strain overestimates the mean strain in the central zone. However, when the strain in the centre of the specimen is considered, the deformation of the transition zones partially compensate for the lower deformation near the shoulders of the specimen.

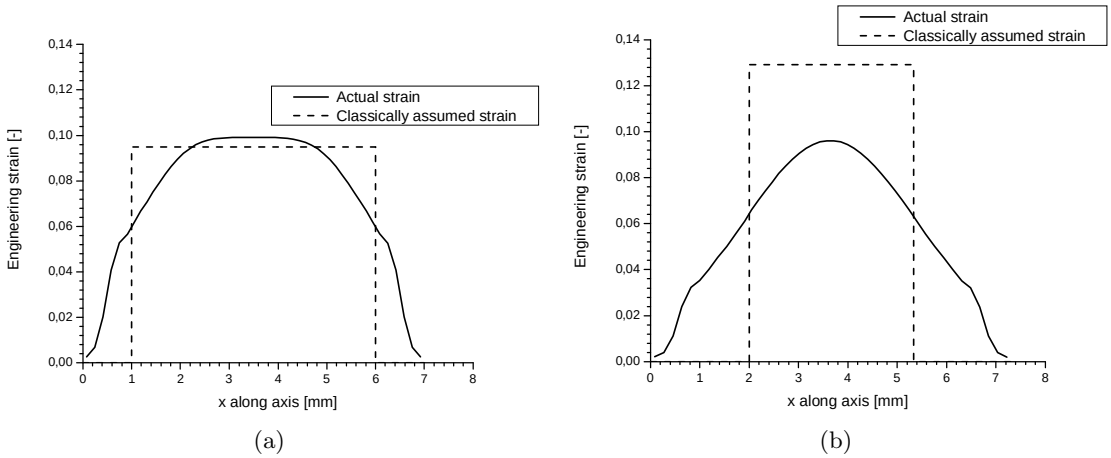


Figure 7 Simulated and classically assumed evolution of the strain along the axis of (a) geometry 3 and (b) geometry 6.

In table 2 the relative overestimation of the classical strain compared with the mean strain in the central zone and with the strain in the centre of the specimen is given for all geometries. The values, calculated at the moment that 10% strain is reached in the centre of the specimen, are in agreement with the trends revealed by the experiments [4]. For all geometries, except geometry 3, the classical strain overestimates the strain in the centre of the specimen; an overestimation of up to 43.9% is reached for geometry 4. The best agreement is obtained for geometry 3: here the classical strain is merely 4.2% lower than the actual strain in the centre. Evidently, the values of table 2 also hold for the strain rate.

6 CONCLUSIONS AND RECOMMENDATIONS

Results of numerical simulations are presented of SHTB experiments considering seven different specimen geometries. The simulations provide information complementary to the experiments and allow an in-depth understanding of the established specimen behaviour.

Table 2 Relative overestimation of the strain in the centre of the specimen and the mean strain in the central zone by the classical strain. These values are calculated at the moment that 10% strain is reached in the centre of the specimen.

Geometry	Classical strain/strain centre at 10% axial strain (%)	Classical strain/mean strain central zone at 10% axial strain (%)
1	20.8	28.2
2	13.9	32.1
3	-4.2	16.9
4	43.9	54.1
5	12.2	17.2
6	34.4	49.4
7	24.9	28.2

It is shown that a Hopkinson experiment does not yield the specimen material response, but the combined response of the specimen (with its specific geometry), the specimen material and the experimental configuration. Commonly neglected non-axial stresses have a major influence on both the specimen response and the accuracy of the classical method used to extract strain and strain rate from the waves recorded during an experiment. These non-axial stresses are dependent on both the geometry and, diameter and material of the Hopkinson bars.

Concerning the assumptions related to the deformation behaviour of the specimen, the simulations confirm the experimental observation that the contribution of the deformation of the transition zones to the total deformation of the specimen is not negligible. Classically, the deformation of the transition zones is added to the deformation of the central zone, resulting in an overestimation of the strain in the central zone. Moreover, further evidence is given that neither the strains, nor the stresses are homogeneous in the central zone of the specimen. Consequently, the history of the stress and the strain of the specimen material is a fictitious notion. Only, in a limited zone around the centre of the specimen, stress and strain can be considered to be homogeneous. The extent of this zone is strongly dependent on geometrical parameters: primarily on the length/width ratio of the central zone, and after that on the radius of the transition zones.

Additional clues are given that a Hopkinson experiment, as generally accepted, cannot provide accurate information on the material behaviour during the early stage of loading. Indeed, 1) the high contribution of the deformation of the transition zones during elastic deformation leads to highly overestimated strain values, 2) structural effects give rise to a delay between the established and actual onset of yielding, 3) the onset of yielding gives rise to the high non-axial stresses in geometries with a low length to width ratio resulting in yield stress levels significantly higher than the actual uniaxial yield stress, and 4) the established deformation values at the early stage of plastic deformation are again determined by both the material and

geometry of the specimen. For all geometries quasi-static equilibrium was established in the early stage of loading.

The choice of the most appropriate specimen geometry is closely related to requirements rising from both fundamental and practical considerations. Since it is the explicit purpose of a Hopkinson experiment to obtain the material response to a uniaxial tensile loading, stresses and strains have to be uniaxial and homogeneous in a sufficiently large zone of the specimen. The major advantage of a Hopkinson experiment is the straightforward calculation of the history of the stress, strain and strain rate in the specimen. Stress and strain are calculated, independently from each other, from measurements on the Hopkinson bars. No complicated and time-consuming measurements on the specimen itself are needed, and no previous assumptions have to be made on behalf of the specimen behaviour. Evidently, it is of utmost importance that the obtained stress and strain histories are an accurate representation of the real stress and strain in a zone around the centre of the specimen where the desired homogeneous, uniaxial stress and strain field is obtained. In view of these requirements, for the material considered here, geometry 3 is the most appropriate specimen geometry: 1) near the centre of the specimen a zone, sufficiently large in view of the microstructural dimensions of metals, exists where the desired stress and strain state is obtained, 2) the deformation of the transition zones is such that it actually allows for the lower deformation near the ends of the central zone, consequently, the classical strain is an excellent and conservative approximation of the strain in a zone around the centre of the specimen and 3) also, the extracted stress history is close to the uniaxial stress level. However, it should be emphasized that the validity of the conclusions is limited to materials having a behaviour resembling the material considered here.

References

[1] H. Kolsky. An investigation of the mechanical properties of materials at very high rates of loading. *Proc. Phys. Soc. Lond*, Sec B, 62:676–700, 1949.

[2] J. Van Slycken, P. Verleysen, J. Degrieck, L. Samek, and B. De Cooman. High-strain-rate behavior of low-alloy multiphase aluminum- and silicon-based transformation-induced plasticity steels. *Metallurgical and materials transactions A-Physical metallurgy and materials science*, 37A(5):1527–1539, 2006.

[3] P. Verleysen and J. Degrieck. Improved signal processing for split Hopkinson bar tests on (quasi-)brittle materials. *Experimental Techniques*, 24(6):31–33, 2000.

[4] P. Verleysen, J. Degrieck, T. Verstraete, and J. Van Slycken. Influence of specimen geometry on split Hopkinson tensile bar tests on sheet materials. *Experimental Mechanics*, 48:587–598, 2008.

[5] S. Walley, W. Proud, H. Goldrein, and C. Siviour. Review of experimental techniques for high rate deformation and shock studies. *International Journal of Impact Engineering*, 30:725–775, 2004.

Latin American Journal of Solids and Structures
www.lajss.org

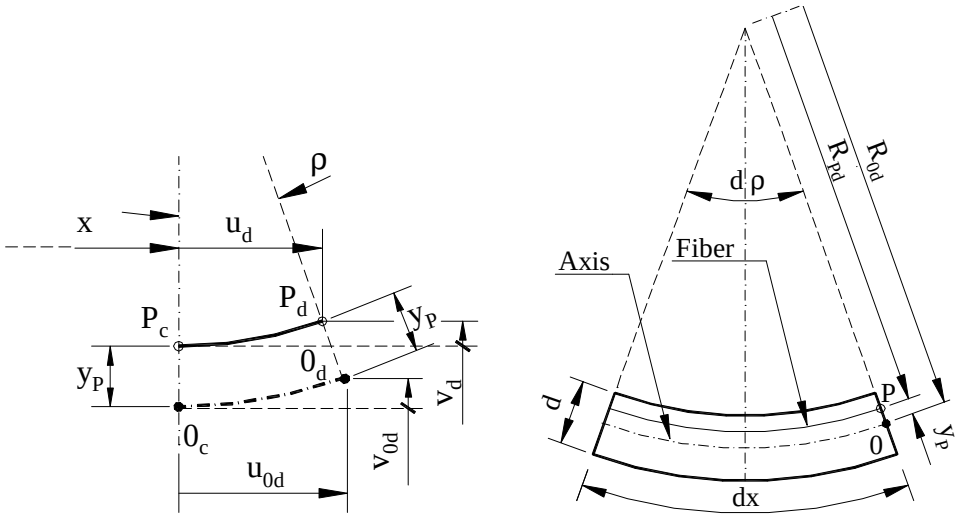
Erratum

Erratum to "Second-order plastic-zone analysis of steel frames, Part I: Numerical formulation and examples of validation"

Latin Amer. J. of Solids and Struct. 6(2) 132–152

Arthur R. Alvarenga and Ricardo A. M. Silveira*
Department of Civil Engineering, School of Mines
Federal University of Ouro Preto (UFOP) Campus Universitário
Morro do Cruzeiro, 35400-000 Ouro Preto, MG – Brazil

The editor regrets that Figure 3 from the above paper was printed wrong and it should be substituted by the one below.



(a) Point P movement related to axis 0. (b) Specific rotation of the fiber.

Figure 3 Fiber and axis relationship.

*Corresponding author email: ricardo@em.ufop.br